JOURNAL OF MATERIALS SCIENCE 12 (1977) 658–665

Magnetic properties of a directionally solidified eutectic alloy containing $Co_{17}Sm_2$ fibres

R. GLARDON, W. KURZ
Département des Matériaux, Ecole Polytechnique Fédérale, Lausanne, Switzerland

An eutectic alloy containing 44% by volume $Co_{17}Sm_2$ fibres has been located in the Co–Sm–Sn system and directionally solidified at speeds of between 1.7 and 550 μm sec^{-1}. The spacing λ, between the fibres and their diameter, d, as a function of the growth rate, R, show the following relations:

$$\lambda^2 R = 42\,\mu m^3\ sec^{-1}$$

$$d^2 R = 10\,\mu m^3\ sec^{-1}.$$

Fibre diameters ranging from 1.6 to 0.14 μm have been obtained and coercive forces of up to 2.3 kOe, for the finest fibres, measured. The behaviour of the coercive force with changing diameter is compared with that in a Bi–MnBi eutectic and in powders made from the same compounds. The results can be interpreted by means of a simple theoretical analysis which shows that the attainment of high coercive forces in powder is restricted by the microscopic surface-defect density introduced during preparation, whilst in eutectics it is limited by the difficulties of growing fine regular structures at high speed.

1. Introduction

The exceptional magnetic properties of the Co_5RE compounds are well known and have led, by means of powder–metallurgical techniques, to the production of a new generation of permanent magnets with much better magnetic characteristics than any other known material. It is also known that the potentially attainable properties of $Co_{17}RE_2$ compounds, and especially those of $(Co,Fe)_{17}Sm_2$, are better again, due to their higher saturation [1]. However, the coercive forces attained so far have been generally only of the order of 2 kOe [2, 3, 4]. Higher coercive forces (up to 8 kOe) have been obtained, but only at the cost of extensive chemical etching of $(Co,Fe)_{17}Sm_2$ powder [3].

The demagnetization of cobalt–rare earth powders is generally believed to be due to the nucleation of reversed domains at defects, the number of which increases with increasing milling time [5]. The weaker coercive fields obtained with $Co_{17}Sm_2$ can be explained by the fact that its critical diameter for single domain behaviour, d_c (for a spherical particle), is smaller than that of Co_5Sm, and, therefore, longer milling times, leading to a greater density of defects, are necessary to reach the same d/d_c ratio [6]. In view of this, the possibility of producing cobalt–rare earth fibres of 1 μm diameter by means of a eutectic reaction, is of great interest. It is probable that single domain particles having these dimensions and obtained by eutectic solidification would exhibit a much lower density of defects than similar particles prepared by milling. The present paper describes a preliminary study of a eutectic alloy containing $Co_{17}Sm_2$ fibres.

2. The alloy and its solidification behaviour

The alloy is a two phase eutectic of the Co–Sm–Sn system. Its microstructure consists of $Co_{17}Sm_2$ fibres (or ribbons, under certain conditions of solidification) in a non-magnetic matrix.

TABLE I

	Co (at.%)	Sm (at.%)	Sn (at.%)
Overall alloy composition	54	28	18
Matrix	8	50	42
Fibres ($\alpha = 0.44$)	88.5	11	0.5

The overall composition of the alloy was determined by X-ray fluorescence analysis and the composition of the individual phases by microprobe analysis.The values obtained for the matrix were doubtful (measured total < 93 wt%) and so the composition of this phase was calculated from the composition of the alloy as a whole, the fibre composition, and the volume fraction, α, of the magnetic phase (Table I). The latter was found by magnetic saturation measurements to be approximately 0.44.

The fibre composition, measured by microprobe analysis, corresponds very closely to that of $Co_{17}Sm_2$ (Co = 89.5, Sm = 10.5% at.) with a small amount of Sn in solution (0.5% at.). It is suggested that the matrix may be a SmSn compound with some 8% at. Co in solution. However, to the authors' knowledge the Sm–Sn phase diagram has never been published so that the existence of this phase remains hypothetical.

The alloy was prepared by melting the pure elements (Co, 99.9; Sm, 99.6 and Sn, 99.9 wt%) together, by induction heating, in a water-cooled copper boat. Unidirectional solidification was carried out in pyrolytic boron nitride crucibles using the Bridgman technique, at speeds of between 1.7 and 100 μm sec^{-1}. The temperature gradient in the furnace was of the order of 150° C cm^{-1}. Non-directionally solidified specimens were also prepared by casting in the water-cooled copper boat.

All specimens exhibited a two-phase structure consisting of fibres or ribbons of $Co_{17}Sm_2$ compound in a non-magnetic matrix of the type $Sm(Sn_{0.84}Co_{0.16})$. Various microstructures were observed, depending on the growth rate. At 1.7 μm sec^{-1}, the structure was regular and contained $Co_{17}Sm_2$ ribbons (Fig. 1). At speeds of between 6.7 and 100 μm sec^{-1} the structure was cellular or dendritic. At the centres of cells, a regular fibrous morphology appeared while in the irregular cell boundaries coarse $Co_{17}Sm_2$ particles (> 10 μm) were present (Fig. 2). Occasionally, large degenerate

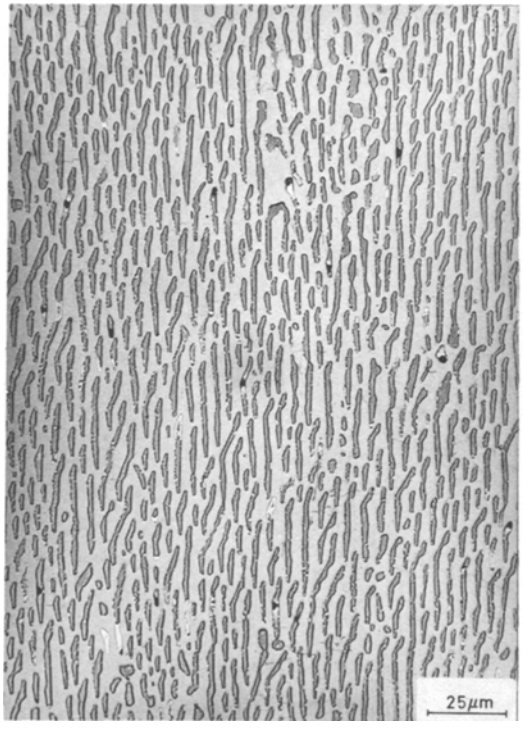

Figure 1 Optical micrograph of the transverse section of a Co–Sm–Sn eutectic alloy directionally solidified at 1.7 μm sec^{-1}.

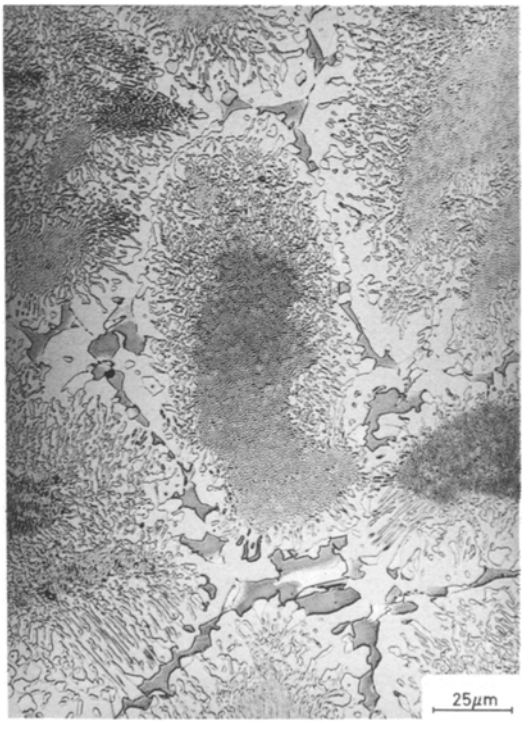

Figure 2 Optical micrograph of the transverse section of a Co–Sm–Sn eutectic alloy directionally solidified at 100 μm sec^{-1}.

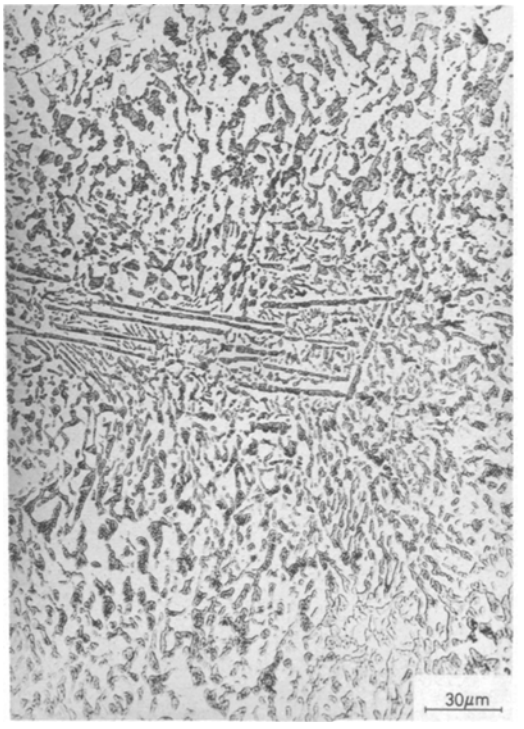

Figure 3 Degenerate structure (transverse section, optical micrograph) of a Co–Sm–Sn eutectic alloy directionally solidified at 27 μm sec^{-1}.

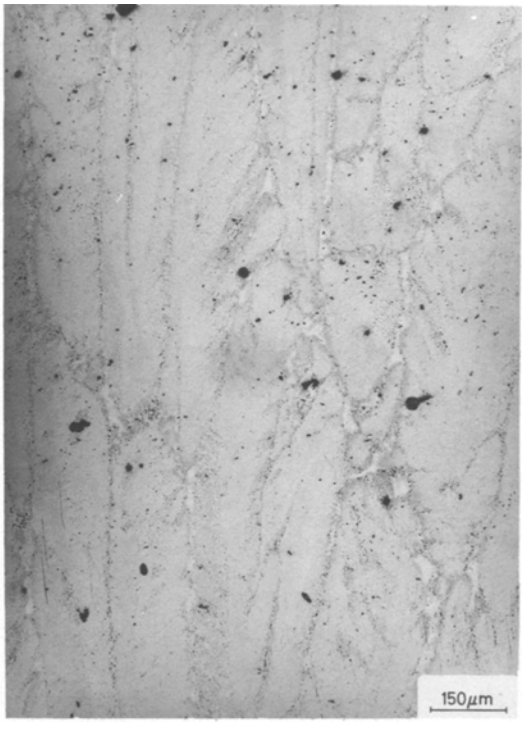

Figure 4 Optical micrograph of a Co–Sm–Sn eutectic alloy chill cast in a water-cooled copper boat (longitudinal section).

zones ($\sim 500\,\mu$m) were observed (Fig. 3). Finally, in chill cast structures (growth rate $\sim 550\,\mu$m sec^{-1}) eutectic dendrites elongated in the direction of heat flow could be seen (Fig.4). On transverse sections of the regular zones of the structure, the fibres exhibited a circular cross-section i.e without facets, for all the growth rates employed except the slowest. The spacing, λ, between the fibres, their diameter, d, and the cell diameter, D, are shown plotted against growth rate, R, in Fig. 5. These parameters obey the following relations:

$$\lambda^2 R = 42\,\mu\text{m}^3\ \text{sec}^{-1}$$

$$d^2 R = 10\,\mu\text{m}^3\ \text{sec}^{-1}$$

$$D^2 R = 2.2 \times 10^6\,\mu\text{m}^3\ \text{sec}^{-1}.$$

At speeds at which cellular or dendritic structures appear, λ and d were measured on the axis of the cell or dendrite. At these points, the local solidification speed corresponds closely to the rate of displacement of the crucible. The relations between λ, d and R were used to estimate the growth rate in the case of the specimen chill cast in the water-cooled boad. The measured diameter, d, of 0.14 μm and the spacing, λ, (0.3 μm for this case) corresponded to a growth rate of about 550 μm

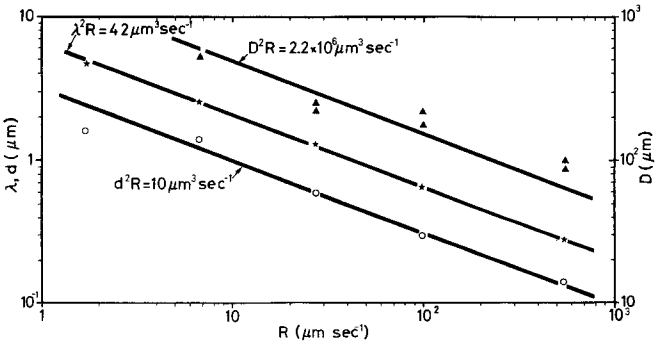

Figure 5 Plot of the interfiber spacing, λ, the fibre diameter, d, and the cell diameter, D, as a function of solidification rate, R.

sec^{-1}. The divergence of the values of λ and d, for growth at $1.7\,\mu m\,sec^{-1}$, from the preceeding relations can be explained by the formation of ribbons rather than fibres at this speed. The greater oxidation losses and reaction with the crucible at this low speed could also play a role.

As indicated above, a uniform structure (planar solidification front) was achieved only at the lowest speed employed, $1.7\,\mu m\ sec^{-1}$. Taking the temperature gradient, G, to be $150^\circ C\,cm^{-1}$, one can therefore, say that the approximate ratio of G/R necessary to maintain a planar solid/liquid interface in this alloy is $\sim 7 \times 10^{-3}\,^\circ C\,sec\,\mu m^{-2}$.

3. Magnetic properties

Demagnetization curves were measured by means of a vibrating sample magnetometer. The degree of magnetic saturation was determined using a torque method after first magnetizing the sample with a field of strength: 17 kOe. The saturation was measured for all specimens and the mean value reached 450 emu cm^{-3}. This value, together with the known saturation, M_s, of the $Co_{17}Sm_2$ compound; 1020 emu cm^{-3} [2] permitted the volume fraction of the magnetic phase to be estimated as being 0.44.

The form of the hysteresis curves seemed to indicate that the easy magnetic axis [0 0 0 1] was oriented perpendicularly to the growth direction at low solidification rates. Fig. 6 shows a longitudinal section of a specimen oriented at $1.7\,\mu m\ sec^{-1}$. The magnetic structure, which is visible in the $Co_{17}Sm_2$ ribbons confirms that the [0 0 0 1] axis was indeed perpendicular to the growth direction. At speeds of between 6.7 and $100\,\mu m\ sec^{-1}$, on the other hand, analysis of the hysteresis curves indicated that the easy axis was parallel to the growth direction. However, as may be seen in Fig. 3, the structures tended to be very badly perturbed, so that these results must be interpreted with caution. After casting in the water-cooled boat at a calculated local growth rate of some $550\,\mu m\ sec^{-1}$, the random orientation gave rise to isotropic magnetic properties so that the crystallographic orientation of the $Co_{17}Sm_2$ fibres could no longer be deduced from the magnetic measurements.

In Figs. 7 and 8, the measured coercive force H_{ci} is shown plotted as a function of fibre diameter, d, and growth rate, R, respectively. The value of H_{ci} increases from nearly zero to about 2300 Oe when R increases from 1.7 to $550\,\mu m\ sec^{-1}$. These values correspond to diameters of between 1.6 and $0.14\,\mu m$ respectively. Since the easy axis of magnetization is perpendicular to the direction of the fibres for solidification at $1.7\,\mu m\ sec^{-1}$, the measured value (nearly zero) of coercive force for this specimen was not taken into account. The demagnetization curves were measured for

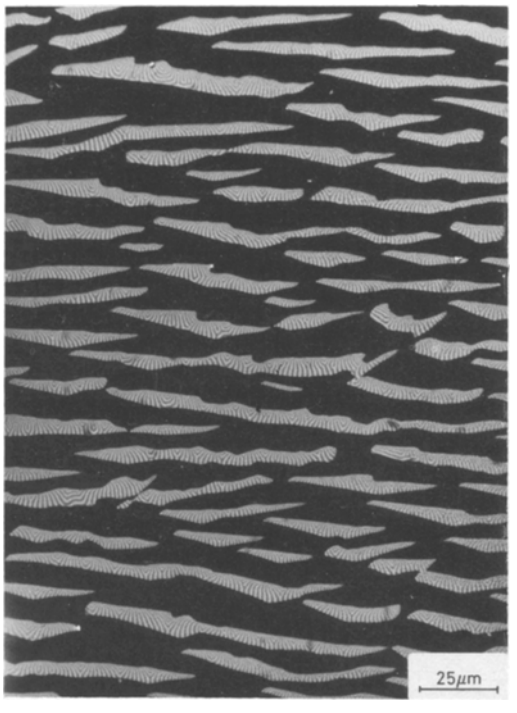

Figure 6 Optical micrograph (polarized light) of the longitudinal section of a Co–Sm–Sn eutectic alloy directionally solidified at $1.7\,\mu m\ sec^{-1}$. The magnetic domain structure visible inside the $Co_{17}Sm_2$ ribbons indicates that the [0 0 0 1] axis is perpendicular to the growth direction.

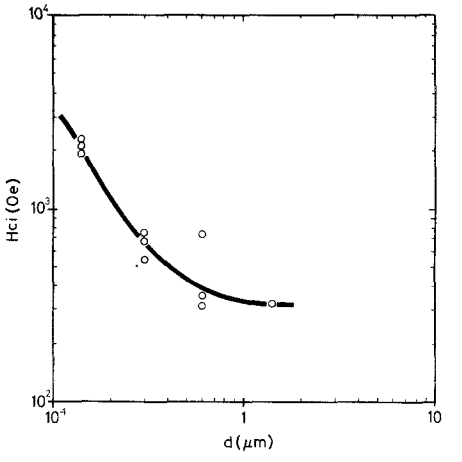

Figure 7 Coercive force, H_{ci}, as a function of the fibre diameter, d.

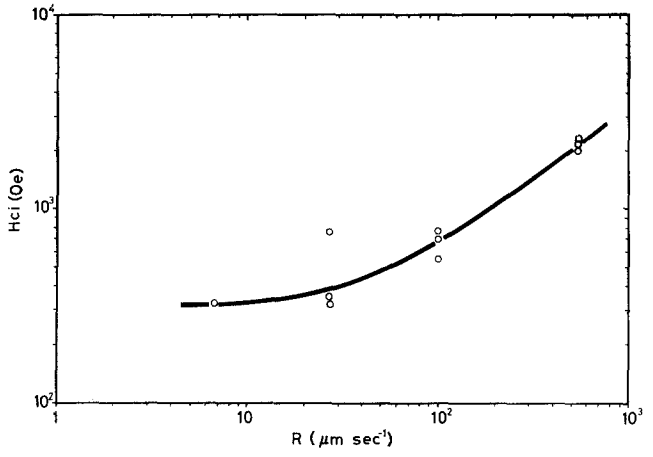

Figure 8 Coercive force, H_{ci}, as a function of the solidification rate, R.

three different directions; one parallel to, and the other two perpendicular to, the growth direction (and to each other). In each case, only the value of H_{ci} measured in the direction closest to that of the easy axis was taken. This was deduced from the form of the hysteresis curve.

4. Discussion

The critical diameter, d_c, for single domain behaviour of a spherical particle of $Co_{17}Sm_2$ is about 0.7 μm [2]. For fibres, however, this value can be much larger. Consequently, the fibres obtained in the present work should be single-domain. In Fig. 9, the measured coercive force is shown plotted against the particle diameter (diameter of a spherical powder particle or of an eutectic fibre) for MnBi [7] and unetched $(Co,Fe)_{17}Sm_2$ powders [2]. Also shown are the results for Bi–MnBi eutectics [7] and for the present work.

The following points can be observed:

(1) The coercive force for MnBi (as a powder or a eutectic alloy) is always higher than for $Co_{17}Sm_2$, although the anisotropy field is much greater for the latter than for the former ($H_a = 65$ kOe for $Co_{17}Sm_2$ and 30 kOe for MnBi). These high coercive forces were obtained for diameters greater than those at which non-zero coercive forces are measured with $Co_{17}Sm_2$.

(2) For both compounds, a significant H_{ci} can be obtained in measurements made on powders with diameters at which H_{ci} for the eutectic is still near zero. This means that, for both compounds, on decreasing d from a high value, a coercive force is obtained in powders first. On further decreasing d, H_{ci} reaches a maximum for powders, while the H_{ci} of the eutectic continues to increase. In other words, the curves for the eutectics are, to some degree, displaced to smaller d (Fig. 9).

(3) A higher H_{ci} can be obtained in the eutectic (at least for $Co_{17}Sm_2$), but only for d values which are very small compared to those for which the maximum H_{ci} is measured in powders.

These points can be considered to be the consequences of two principle causes: (a) macroscopic (in relation to the fibre diameter) irregularities in the eutectic alloys, and (b) microscopic defect dis-

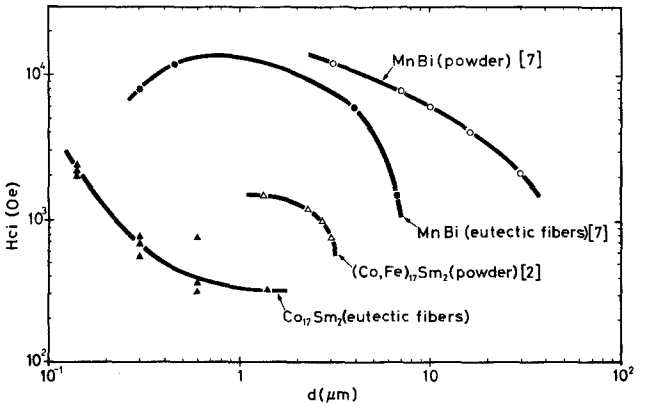

Figure 9 Coercive force, H_{ci}, as a function of the eutectic fibre or powder particle diameter for MnBi and $Co_{17}Sm_2$ compounds.

tribution in small magnetic particles (powder or eutectic fibres).

4.1. Structure irregularity and degeneration

As can be seen from Figs. 2 and 3, irregularities in the structure lead to the formation of large particles and to a lack of alignment. This latter phenomenon is supposed to increase in importance with increasing growth rate and to give rise to a decrease in the coercive field. Such an explanation was used by Boulbes and others to explain the curve for Bi–MnBi eutectics [7] (Fig. 9). In this respect it must be noted that all of the values reported here for the $Co_{17}Sm_2$ eutectic fibres can be expected to be higher for more regular structures. Although the effect of structure may be important at certain rates of growth, it cannot explain the disparity observed between the H_{ci} values of slowly grown, regular eutectic structures and powder of the same nominal diameter as the eutectic fibres.

In the case of MnBi–Bi eutectics, the increasing part of the curve was assumed to be due to the onset of single-domain behaviour. However, no reasons for the discrepancy observed with MnBi powders were given [7].

4.2. Microscopic defect distribution on small particles

The demagnetization of the small particles used by Boulbes and others, and the demagnetization of the materials in the present study, is believed to be controlled by a reversed domain nucleation phenomenon. This assumption is probably correct because the measured coercive forces are small compared to the anisotropy fields. The demagnetization cannot, therefore, occur by a coherent rotation or even by a curling mode.

In his micromagnetic theory, Brown [8] treats the case of nucleation at surface defects. He shows that the number of defects present in a finite surface area is a random variable having a Poisson distribution. The mean number $\bar{N}$ of defects in an area, S, is then

$$\bar{N} = \nu S \qquad (1)$$

where ν is the mean number of defects per unit of surface area. The probability that the particle contains no defect is then:

$$P_o = e^{-\nu S}. \qquad (2)$$

The coercive force of a particle should vary in the same way as P_o does, having its maximum value (theoretically, $H_{ci} = H_a$) when P_o tends to unity and approaching zero when P_o tends to zero (i.e. when the particle contains a lot of defects). P_o can thus be considered as a measure of the coercive force for a single-domain particle. It should be noted that this equation relating P_o to H_{ci} may have to be modified in the case of very small diameters, due to the appearance of superparamagnetism. However, for $Co_{17}Sm_2$ and MnBi, the critical diameter at which this phenomenon becomes apparent is so small (~ 50 Å at room temperature) that it can safely be ignored.

A value of $\nu = 1.7 \times 10^3$ cm^{-2} is calculated by Brown from data on whisker experiments. He then uses this value to show that a particle of surface area equal to 10^{-8} cm^2 (i.e. a diameter of about 1 μm) has a P_o value very near to unity and is thus practically certain to be free of defects. This derivation is unconvincing because a value of ν calculated from whisker experiments can obviously not be used to estimate the defect density in particles obtained by milling. It is suggested here that ν is not a constant but depends on both the material and the process. This is confirmed by the increasing defect density observed during the comminution of $Co_{17}Sm_2$ powders and the fact that the coercive force can be markedly increased by etching [3].

To explain the form of Fig. 9 where H_{ci} is plotted against d, P_o must be expressed in terms of the particle diameter. This gives the following equations:

spherical particle:

$$S = \pi d^2 \qquad P_o = e^{-\pi\nu d^2} \qquad (3)$$

eutectic fibres:

$$S = \pi d l \simeq 10^3 \pi d^2 \quad P_o = e^{-10^3 \pi\nu d^2} \qquad (4)$$

where $l \simeq 10^3 d$ is the fibre length.

To a first approximation, ν can be thought of as being independent of d for eutectics, assuming that the defect density of the fibres does not depend on the growth rate. In the case of powders on the other hand, ν varies with the particle size; increasing very strongly with decreasing diameter as pointed out above. From equations 3 and 4, P_o can be plotted against d for different cases.

This has been done schematically in Fig. 10, where P_o is shown for eutectics and powders with

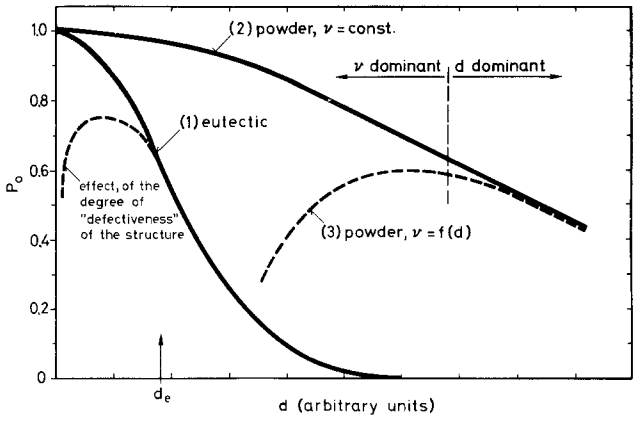

Figure 10 Probability, P_o, that a small magnetic particle contains no defects, as a function of particle diameter, d.

ν taken as a constant. Curve 3 of the same figure shows a schematic variation of P_o for powders when ν increases with decreasing diameter. On this latter curve, two parts can be distinguished: one applying to large diameters, where the d term of Equation 3 is dominant, and the second to small diameters where the ν term is dominant, leading to a decrease in P_o for small d.

Returning now to Fig. 9, the diverse characteristics observed can be explained by reference to Fig. 10:

(1) The higher value of H_{ci} for MnBi at larger diameters (powder or eutectic fibres) could be due to a more elevated value of ν for $Co_{17}Sm_2$ than for MnBi. This implies that for identical conditions (geometry and process), $Co_{17}Sm_2$ must contain a greater defect density than MnBi.

(2) The fact that on decreasing d, a coercive force first appears for powders and its value reaches a maximum while the value for eutectic fibres continues to increase can clearly be explained by a comparison of the curves 1 and 3 in Fig. 10: due to the much smaller (by a factor of about 10^3 for the same diameter) surface area of powders, P_o (powder) is much higher than P_o (eutectic) for a given d. On the other hand, since ν has been assumed to be a constant for eutectics and to vary with diameter for powders, P_o (powder) must reach a maximum and then decrease, while P_o (eutectic) monotonically increases. As was indicated earlier, an eventual decrease of H_{ci} for eutectics can be attributed to structural modifications (Fig. 10).

(3) The higher H_{ci} measured for eutectic fibres of small diameter compared to powders can be explained in the same way by comparing Curves 1 and 3 of Fig. 10. It can be seen that if a sufficiently small fibre diameter (d_e in Fig. 10) could be obtained (without too great a structural modification) larger values of P_o would be obtained for eutectics as compared to the maximum for powders (Curve 3).

Thus, the characteristic variations of H_{ci} for powders and eutectics based on $Co_{17}Sm_2$ and MnBi can be interpreted by a consideration of the combined effects of structural irregularities and the defect distributions on the surface of small particles. It should be noted that this analysis is not confined to these compounds alone but can be applied to other small particles.

5. Conclusion

A simple theoretical analysis shows that the use of eutectic alloys containing highly anisotropic magnetic fibres should lead to the attainment of high coercive forces. It is shown that this latter characteristic is limited, in the case of powders, by the increase in microscopic surface-defect density of the grains with decrease in size. On the other hand, the coercive force obtainable with eutectic alloys seems to be restricted by the production of regular aligned structures at high solidification rates.

The first point above has been to some extent confirmed by experimental results on eutectic alloys comprising $Co_{17}Sm_2$ fibres which indicate a value of H_{ci} of 2.3 kOe. Although this value is still very small compared to the theoretical limit (~65 kOe), it shows that eutectics could represent and interesting way of trying to approach it.

The eutectic alloy studied here, which has a saturation magnetization of about 450 emu cm^{-3} (theoretical $BH_{max} \sim 8$ POe)* is probably of little commercial interest due to its high samarium con-

*1 POe = 10^{15} Oe.

tent (44% wt) but nevertheless it could be used as a means of experimenting on very fine particles of $Co_{17}Sm_2$. The information thus obtained could then be useful in the preparation of permanent magnets by other means.

Acknowledgements

The authors are grateful to Mr G. Buri and Mr Mahé (University of Lausanne) for the great care taken in carrying out the microprobe analysis. Thanks are also due to Mr C.-A. Jeanneret (Fabriques d'Assortiment Réunies, Division R, Le Locle) for performing the magnetic measurements and to Mr J.-P. Schneider for technical assistance throughout. We are very grateful to Dr J. D. Livingston (General Electric Corporate Research & Development, Schenectady) for critical remarks and careful reading of the manuscript. This work was carried out with the financial support of the Fabriques d'assortiments Réunies, Division R, Le Locle.

References

1. K. J. STRNAT, *IEEE Trans. Mag.* MAG-8 (1972) 511.
2. R. S. PERKINS, S. GAIFFI and A. MENTH, *ibid* MAG-11 (1975) 1431.
3. V. Y. BRYANTSEV, V. V. SERGEYEV, G. V. MALAKHOV amd V. K. SLIDCHENKO, unpublished results.
4. J. P. HEINRICH and H. GARRETT, J. Appl. Phys. 45 (1974) 1873.
5. J. D. LIVINGSTON, AIP Conf. Proc. No. 10 (1972) 643.
6. J. D. LIVINGSTON and M. D. McCONNELL, *J. Appl. Phys.* 43 (1972) 4756.
7. J. C. BOULBES, R. W. KRAFT and M. R. NOTIS, Proceedings of the Conference on *In Situ* Composites, Lakeville III (1972) p. 61.
8. W. F. BROWN, "Micromagnetics", (Interscience, New York, 1963).

Received 23 August and accepted 10 September 1976.